



Interacting electrons on a two-dimensional surface: planar vs. spherical geometries

Arkadiusz Wójs*, John J. Quinn

Department of Theoretical Physics, The University of Tennessee, Knoxville, TN 37996-1501, USA

Received 2 July 1998; accepted 8 July 1998

Abstract

The center-of-mass excitations are identified in the spectrum of electrons on a two-dimensional surface in the lowest Landau level. The correspondence between the quantum numbers labeling electron states on a sphere and on a plane is drawn. The excitation spectrum on a sphere with increasing radius is shown to converge to that on a plane. In particular, in the presence of a lateral confinement (i.e. for the case of quantum dots), identical series of magic states appear in both cases. Also, a class of interaction potentials which lead to the fractional quantum Hall effect in an extended system are identified. © 1998 Elsevier Science B.V. All rights reserved.

PACS: 73.20.Dx; 73.40.Hm

Keywords: Electron interactions; Two-dimensional surface

1. Introduction

The discovery of the fractional quantum Hall effect (FQHE) [1] raised great interest in the properties of interacting two-dimensional electron gas (2DEG) in high magnetic fields. In the degenerate lowest Landau level (LL), the electron–electron (e – e) interaction cannot be treated perturbatively. Instead, numerical diagonalization techniques have often been used, which, however, limit the system to a finite (small) number of electrons. In order to model an extended 2DEG by a finite system, electrons can be put on a closed surface (sphere) [2]; alternatively,

a lateral (parabolic) potential [3] or periodic boundary conditions (PBC) [4] can be used on a plane. While all these approaches aim at the description of the same 2DEG system, different geometry leads to different symmetries, different finite-size effects, etc. Analysis of the excitation spectra shows that different sets of good quantum numbers appear in different cases: e.g., total angular momentum and its projection on a sphere, and center-of-mass (CM) and relative (REL) angular momentum projections on a plane in the circular gauge.

In this paper we shall explore the correspondence between these sets of quantum numbers and demonstrate that the underlying CM symmetry appears for a 2DEG on both surfaces. The resulting similarities between the excitation spectra on both surfaces will

* Corresponding author. Permanent address: Institute of Physics, Wrocław University of Technology, Wybrzeże Wyspiańskiego 27, 50-370 Wrocław, Poland.

be pointed out. Also, we shall study the effect of the form of e–e repulsion on the excitation spectrum; particularly on the occurrence of incompressible ground states (GS's) at the fractional filling factors known in the context of the FQHE.

On a plane, electrons confined by a lateral potential were also used as a model of experimentally realizable systems called *quantum dots*, where a few electrons are indeed bound in a small area [5]. In analogy, we shall study a spherical model of a quantum dot, where electrons are confined around a pole. In both models (on a sphere and on a plane), a lateral confinement of varied strength will be shown to drive the 2DEG through the same sequence of magic states.

2. Model and single-particle states

The system of N interacting electrons moving on a smooth 2D surface and subject to a magnetic field \mathbf{B} perpendicular to the surface is considered. The intensity of the field, B , is constant. As specific examples, two surfaces: a plane and a sphere, will be discussed. Within the surface, a lateral potential V_L confines the system to a finite area, a quantum dot. The total single-particle (SP) hamiltonian, i.e. both the geometrical constraint defining the surface and the lateral confinement, are assumed to be rotationally symmetric around the z -axis. We assume the Zeeman gap to spin-polarize the electron gas in both cases, so that the spin degree of freedom can be ignored.

In the absence of a lateral confinement, the SP energies, ε_{nm} , form degenerate LL's separated by gaps of the order of the cyclotron energy, $\hbar\omega_c = eB/\mu c$ (e and μ are electron charge and effective mass, respectively), and labeled by the LL index $n = 0, 1, \dots$. The states within each (n th) spin-polarized LL, $|n, m\rangle$, are labeled by the projection of orbital angular momentum, m . We shall discuss the strong field limit, i.e. neglect the LL mixing due to the lateral confinement and/or e–e interaction. The SP states in the lowest, spin-polarized LL are denoted by $|m\rangle$, and their energy is $\varepsilon_m = \frac{1}{2}\hbar\omega_c$.

The lateral (quantum-dot) confinement V_L removes degeneracy of the lowest LL. It will be chosen in such a form, that the dispersion is linear, $\varepsilon_m = \frac{1}{2}\hbar\omega_c - m\Delta$.

The eigenstates in the presence of V_L are the same as without V_L , since without the LL mixing ($\Delta \ll \hbar\omega_c$) each SP m -subspace contains only one state, $|m\rangle$.

The particular forms of the hamiltonian which give the model SP spectrum postulated above in cases of planar and spherical surfaces are presented below.

On a plane, the magnetic field perpendicular to the surface is a uniform field, $\mathbf{B} = B\hat{z}$. The lateral potential that gives a linear dispersion of LL's is an isotropic harmonic well, $V_L(x, y) = \mu\omega_0^2(x^2 + y^2)/2$. The SP eigenstates are those of a pair of uncoupled harmonic oscillators, $|n, m\rangle = (a^+)^n(b^+)^{n-m}|0, 0\rangle/\sqrt{n!(n-m)!}$. The energies are $\varepsilon_{nm} = \hbar\omega_+(n + 1/2) + \hbar\omega_-(n - m + 1/2)$, where $\omega_{\pm} = (\Omega \pm \omega_c)/2$ and $\Omega^2 = \omega_c^2 + 4\omega_0^2$. In high magnetic fields, the intra-LL excitation energy is $\Delta = \hbar\omega_- \approx \hbar\omega_0^2/\omega_c$ and the inter-LL separation is $\hbar\Omega \approx \hbar\omega_c$. The LL mixing at a finite $\omega_- : \omega_+$ ratio replaces the magnetic length $l_B = \sqrt{\hbar c/eB}$ by a new length scale, $l_0 = \sqrt{\omega_c/\Omega} l_B$. The lowest-LL wavefunctions, $\langle \mathbf{r} | m \rangle$, correspond to circular orbits with increasing radii $\approx \sqrt{m} l_B$ (the flux through the area inside the orbit is $m\phi_0$, where $\phi_0 = hc/e$ is the flux quantum).

On a sphere, the magnetic field perpendicular to the surface is an isotropic radial field, $\mathbf{B} = \pm B\hat{\Omega}$ (here, $\hat{\Omega} = \mathbf{r}/r$ is the radial versor), produced by a magnetic monopole of strength $2S$ placed at the origin. The total flux through the sphere of radius R is $4\pi BR^2 = 2S\phi_0$ (i.e., $R^2 = S l_B^2$); positive S means \mathbf{B} pointing outwards. $2S$ is an integer, as required by Dirac's monopole quantization condition. In the absence of a lateral confinement, the SP states (monopole harmonics) are the eigenstates of the angular momentum, l , and its projection, m , with the LL index $n = l - S$ [6]. The angular momentum ladder operators $l^{\pm} = l_x \pm i l_y$ connect states within each LL, $|n, m\rangle = \sqrt{(l+m)!/(l-m)!/(2l)!} (l^-)^{l-m} |n, l\rangle$. The energy levels are $\varepsilon_{nm} = \hbar\omega_c [n + 1/2 + n(n+1)/2S]$. The lowest-LL wavefunctions, $\langle \mathbf{r} | m \rangle$, correspond to circular orbits around the z -axis, at the height $\langle z/R \rangle \approx m/(S+1)$.

The lateral potential V_L that gives a linear dispersion of LL's on a sphere (in analogy to a quantum dot on a plane) is linear in z , $V_L(z) = -(S+1)\Delta z/R$. For $S > 0$, V_L confines electrons around the north pole ($z = R$). It follows from the orthogonality of Jacobi polynomials that the only nonvanishing matrix

elements are the diagonal ones and those between the neighboring LL's:

$$\langle n, m | z/R | n, m \rangle = \frac{S}{l(l+1)} m, \quad (1)$$

$$\langle n-1, m | z/R | n, m \rangle = \sqrt{\frac{(l^2 - m^2)(l^2 - S^2)}{l^2(4l^2 - 1)}}. \quad (2)$$

The LL mixing due to the off-diagonal terms in V_L is fairly weak and the resulting deviations from the linear dispersion are negligible even when neighboring LL's begin to overlap, i.e. for $2l\Delta \approx \hbar\omega_c$.

3. Center-of-mass excitations within the lowest Landau level

The total many-particle (MP) hamiltonian contains the SP and e–e (Coulomb) interaction terms that commute with each other:

$$H = \sum_m \varepsilon_m c_m^\dagger c_m + \frac{1}{2} \sum_{m_1 m_2 m_3 m_4} \langle m_1 m_2 | V_C | m_3 m_4 \rangle c_{m_1}^\dagger c_{m_2}^\dagger c_{m_3} c_{m_4}. \quad (3)$$

Operators c_m^\dagger (c_m) create (annihilate) an electron in the state $|m\rangle$, and $\langle m_1 m_2 | V_C | m_3 m_4 \rangle$ are the two-body interaction matrix elements (for a plane cf. Ref. [7]; for a sphere cf. Ref. [8]).

The MP Hilbert space is spanned by SP configurations, $|m_1, m_2, \dots, m_N\rangle = c_{m_1}^\dagger c_{m_2}^\dagger \dots c_{m_N}^\dagger |\text{vac}\rangle$, where $|\text{vac}\rangle$ stands for vacuum. Each basis configuration is classified by the projection of the total angular momentum, $M = \sum_{i=1}^N m_i$, and thus also by the SP energy, $E^{\text{SP}} = N\hbar\omega_c/2 - M\Delta$. The eigenstates $|\phi\rangle$ of the total hamiltonian H are these of the interaction V_C alone. They are obtained through the diagonalization, separately for each M -eigensubspace. The eigenenergies, E_ϕ , are the eigenenergies of interaction, E_ϕ^C , shifted by appropriate SP energies, E_ϕ^{SP} . The total angular momentum will be denoted by L (on a plane it is trivially $L = |M|$).

If the confinement, scaled by Δ , prevails over the e–e repulsion, and at the same time the cyclotron gap prevents scattering to higher LL's, the GS of the MP system is a *compact droplet* (CD) corresponding to

the filling factor $\nu = 1$ [9–11]. The CD is a *noninteracting* configuration, in which electrons occupy consecutive SP orbitals around the minimum of V_L , up to a Fermi level, $|\text{CD}\rangle = (\prod_{m \geq m_F} c_m^\dagger) |\text{vac}\rangle$. Since it is the only MP state in the Hilbert space with its total angular momentum projection, M_{CD} , it is an *exact* eigenstate of the interacting hamiltonian H . Also, $L_{\text{CD}} = |M_{\text{CD}}|$.

When the confinement strength (Δ) falls down to a critical value, the e–e repulsion induces a GS transition (reconstruction of the CD). Further decrease of Δ leads to the subsequent changes of the MP GS through a series of states with increasing area, i.e. increasing M [10,11]. Only certain (*magic*) values of M appear in the series, known in the context of quantum dots on a plane [3,11–13]. Below, we analyze the excitations which connect different M -spaces and thus also different magic GS's. We shall concentrate on the relation of these excitations to the CM and REL motions.

3.1. General surface

Within an isolated, n th LL (e.g. the lowest LL), a class of excitations can generally be constructed which do not change the e–e interaction energy; they are the CM excitations. In the absence of a lateral confinement V_L , the SP energy is a number and can be eliminated by a gauge transformation. The total n th-LL hamiltonian, $H_n = V_C$, depends only on the REL positions, $\mathbf{r}_{ij} \equiv \mathbf{r}_i - \mathbf{r}_j$, and does not depend on the CM position, $\mathbf{R} = \sum_{i=1}^N \mathbf{r}_i/N$. Thus, the excitations associated with the CM degree of freedom do not couple to H_n . Even though \mathbf{R} does not explicitly appear in H_n , the spectrum of CM excitations is not that of a free particle due to the restriction of SP states to a single LL, specific for a given surface. In general, for a given eigenstate $\phi(\mathbf{r}_1, \dots, \mathbf{r}_N)$, the Hilbert space \mathcal{H}_ϕ of states different from ϕ by a CM excitation is the projection of the space \mathcal{H}_ϕ^0 , which corresponds to the free CM motion and is spanned e.g. by $\{e^{i\mathbf{P}\mathbf{R}/\hbar} \phi\}_{\mathbf{P}}$, onto the n th LL on a given surface, $\mathcal{H}_\phi = \mathcal{P}_n \mathcal{H}_\phi^0$. By definition, \mathcal{H}_ϕ includes states ϕ' that have identical pair correlation function, $G_{\phi'}(\mathbf{r}) = G_\phi(\mathbf{r}) \equiv \langle \phi | \delta(\mathbf{r}_{1,2} - \mathbf{r}) | \phi \rangle$, and thus can be written as $\phi' = \psi(\mathbf{R})\phi$. Since the number of SP states in each LL is countable, so is the

number of states in \mathcal{H}_ϕ . If the LL degeneracy is finite (closed surface), so is that of \mathcal{H}_ϕ .

Any lateral confinement that contains only terms linear in components of \mathbf{r} , \mathbf{p} , \mathbf{r}^2 , \mathbf{p}^2 , or $\mathbf{l} = \mathbf{r} \times \mathbf{p}$, can be split into the sum of CM and REL parts, and does not affect the CM–REL decoupling [14] (however, it will lead to a nonzero CM excitation energy). In the limit of $\Delta \ll \hbar\omega_c$ (within a single LL) we have $V_L \approx \text{const} - l_z \Delta$, and the decoupling holds for any rotationally symmetric surface. (In the special case of a plane, it also holds in the presence of LL mixing; the Kohn theorem [15].)

Let us write the explicit form of the CM-excitation creation operator [12]. The n th LL is spanned by the SP states $|m\rangle$. These states are connected with a ladder operator, $q = \sum_m |m\rangle\langle m+1|$. In particular, on a plane: $q = b^+$, and on a sphere: $q = l^-$. The MP excitation in form of the sum over all particles, $Q = \sum_{i=1}^N q_i = \sum_m c_m^+ c_{m+1}$, decouples from the REL motion,

$$[\mathbf{r}_{ij}, Q] = 0. \quad (4)$$

Also, $[M, Q] = -Q$ and $[H, Q] = \Delta Q$, and hence Q carries $M = -1$ and SP energy Δ . (Note that the axial symmetry of hamiltonian H is not necessary for the construction of Q and the CM excitations; it is sufficient if the SP energy spectrum is linear in a single, discrete quantum number.) Thus, for a given MP eigenstate $|\phi\rangle$ with $M = M_\phi$ and $E = E_\phi$, a ladder of states can be constructed, $|\phi_k\rangle = Q^k |\phi\rangle$, with $M = M_\phi - k$ and $E = E_\phi + k\Delta$. Also, each eigenstate of the total MP hamiltonian H can be uniquely decomposed, $|\phi_k\rangle = Q^k |\phi_0\rangle$, where $|\phi_0\rangle$ is a *pure REL state*, defined as $Q^+ |\phi_0\rangle = 0$. Clearly, as follows from the commutation (4), Q does not change the pair correlation function, $G_{\phi_k} = G_{\phi_0}$, and thus $\phi_k = \psi_k(\mathbf{R})\phi_0$.

The states connected with Q belong to different Hilbert M -spaces, and each M -space splits into eigensubspaces of states with a defined number of Q -excitations. None of the Q -excited states falls into the magic sequence of GS's.

For example, in the case of three electrons on a sphere at $2S = 8$, the SP angular momentum is $l = 4$, the allowed values of total angular momentum are $L = 1, 3, 4, 5, 6, 7$, and 9, and the space of $L = 3$ is 2D (symbolically, the total Hilbert space decomposes into $1 \oplus 3^2 \oplus 4 \oplus 5 \oplus 6 \oplus 7 \oplus 9$). There are 8 *nondegenerate* pure REL states, two of which have $L = 3$

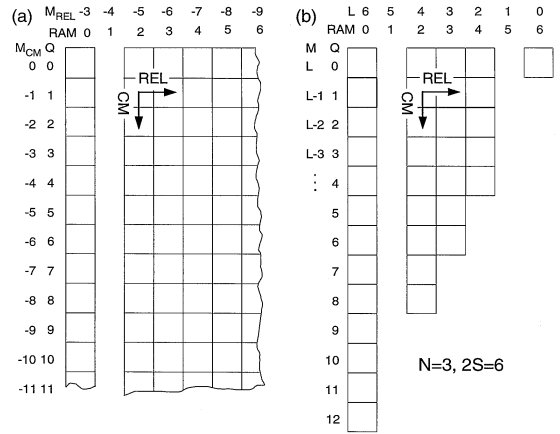


Fig. 1. Schematic picture of CM–REL Hilbert spaces of three electrons; (a) plane; (b) sphere, $2S = 6$.

(the pair of eigenstates in the 2D space with $L = 3$ depend on the specific form of e–e interaction). To each pure REL state the CM excitations can be independently attached. In particular, acting with Q on each of the two pure REL states in the $L = 3$ space generates an independent ladder of states (cf. also Fig. 1 for $2S = 6$).

3.2. Special cases: plane vs. sphere

On a plane, $q = b^+$ is linear in x, y, p_x , and p_y , and thus Q is linear in CM variables, $Q = [(X - iY)/l_0 - 2(\partial_X - i\partial_Y)l_0]/2\sqrt{2}$. Operator Q decreases CM angular momentum projection, $M_{\text{CM}} = [\mathbf{R} \times \mathbf{P}]_z$. The difference $M_{\text{REL}} = M - M_{\text{CM}}$ describes motion relative to the CM and remains untouched by Q . The pair M_{CM} and M_{REL} are good quantum numbers. A special property of the plane (trivial constraint, $z = 0$) and of the parabolic confinement V_L is that the total hamiltonian H is simply a sum of CM and REL hamiltonians, $H = H_{\text{CM}} + H_{\text{REL}}$, and hence the total Hilbert space is a simple product of CM and REL Hilbert spaces.

On a sphere, $q = l^-$ and $Q = L^- \equiv L_x - iL_y$ reduces the total angular momentum projection L_z without changing the length L (L and L_z are good quantum numbers). As follows from the proceeding general discussion, this is a CM excitation. However, due to

the nontrivial constraint, $x^2 + y^2 + z^2 = R^2$, the total Hilbert space is *not* a simple product of CM and REL Hilbert spaces. In consequence, e.g., for a pair of different pure REL states, $\phi \neq \phi'$, the CM-excitation prefactors ψ and ψ' ($Q\phi = \psi\phi$ and $Q\phi' = \psi'\phi'$) need not be equal. Moreover, the numbers of CM excitations that can be attached to ϕ and ϕ' are, in general, different. In other words, the CM excitations do not affect the REL motion, but the REL excitations (e.g. between different pure REL states) couple to the CM motion.

Let us now compare the planar (P) and spherical (S) systems: (P) open surface \rightarrow infinite LL degeneracy, $0 \geq m \geq -\infty$; (S) closed surface \rightarrow finite LL degeneracy, $0 \geq m - S \geq -2S$. In order to unify notation, a pair of new quantum numbers, \mathcal{L} and \mathcal{Q} , are defined: (P) $\mathcal{L} = |M_{\text{REL}}|$ and $\mathcal{Q} = |M_{\text{CM}}|$; (S) $\mathcal{L} = L$ and $\mathcal{Q} = L - M$. \mathcal{L} labels pure REL states and \mathcal{Q} gives the number of CM excitations attached to a pure REL state. The dimension of the space of pure REL states with a given \mathcal{L} depends on \mathcal{L} , electron number N and the LL degeneracy. Further, it is convenient to replace \mathcal{L} by the *relative angular momentum*, $\text{RAM} = |\mathcal{L} - L_{\text{CD}}|$, which measures \mathcal{L} relative to that of the CD (modulus is needed, because $\mathcal{L} \geq L_{\text{CD}}$ on P, and $\mathcal{L} \leq L_{\text{CD}}$ on S). The CD has $\text{RAM} = 0$, and higher RAM means that the electrons occupy a larger area of the surface (as will be shown later, RAM measures the average squared e–e distance). The number of RAM-spaces: (P) infinite, $0 \leq \text{RAM} \leq \infty$; (S) finite, $0 \leq \text{RAM} \leq L_{\text{CD}}$. The maximum number of CM excitations that can be attached to a pure REL state: (P) infinite, $0 \leq \mathcal{Q} \leq \infty$; (S) finite, depends on RAM, $0 \leq \mathcal{Q} \leq 2\mathcal{L}$. The Hilbert spaces (RAM, \mathcal{Q}) for a plane and a sphere ($2S = 6$) have been schematically drawn in Fig. 1 for the case of three electrons. Nonempty spaces are shown as squares. In this picture, the CM excitations are vertical; the top row are pure REL states, and the REL excitations are horizontal.

Generally, the SP energy can be expressed through RAM and \mathcal{Q} as follows: $E^{\text{SP}} = N\hbar\omega_c/2 + (\text{RAM} + \mathcal{Q} - M_{\text{CD}})\Delta$. The first term is the lowest LL energy. The second term is a straight line vs. RAM and gives the SP energy of REL excitations. The third term is the CM-excitation energy, and since only states without CM excitations can be GS's (at an appropriate value of $\Delta > 0$), we can neglect all other states and

set $\mathcal{Q} = 0$. The fourth term is a constant, the SP energy of the CD. The interaction energy depends only on RAM.

As follows from the above comparison that there are two major qualitative differences between the planar and spherical cases:

(i) A plane is an open surface, with infinite LL degeneracy and no constraint on the magnitude of the magnetic field. On the contrary, the LL degeneracy for closed surfaces is finite, and the total magnetic flux through the surface is quantized.

(ii) A plane is a flat surface, where the angular momentum (\mathbf{L}) algebra is 1D ($L = |M|$). The trivial geometrical constraint does not introduce coupling between CM and REL motions, and each of them can be attributed to its own 1D \mathbf{L} -algebra. Thus the MP states can be classified with a pair of *independent* quantum numbers, e.g., M and M_{CM} (it is not important here whether their operators commute with H). On the contrary, on any curved surface (e.g., a sphere) the \mathbf{L} -algebra is 3D. However, the additional degree of freedom associated with the orientation of \mathbf{L} appears at a cost of CM–REL coupling introduced inherently by the nontrivial geometrical constraint. Thus, from the four quantum numbers, L , M , L_{CM} , and M_{CM} , only two are independent. As it follows from our discussion above, the pair of *good* quantum numbers, RAM and \mathcal{Q} , can be always constructed, which have the same physical meaning as their planar counterparts.

4. Magic states on a plane and on a sphere

As an illustration of the similarity between electron systems on different surfaces, it is shown in this section for the example of six electrons how the excitation spectra on a sphere converge to that on a plane when the sphere radius, R , is increased. Since B on the surface is fixed and $R^2 = S l_B^2$, an increase of R is achieved by increasing S . The lowest interaction eigenenergy in each RAM-subspace, $E^{\text{C}}(\text{RAM})$, has been plotted in Fig. 2 for a sphere (dots, $2S = 7, 8, \dots, 20, 25, 30, 35$, and 50) and a plane (squares). The sequence of magic RAM's can be identified at the downward peaks; these will be the GS RAMs at appropriate strengths of confinement. The vertical lines show magic RAMs for

a plane.¹ The unit of energy in Fig. 2 is chosen as the interaction energy for two electrons occupying the same, innermost orbital, i.e. $\langle 00|V_C|00\rangle$ on a plane, and $\langle SS|V_C|SS\rangle$ on a sphere.

The definition of RAM makes the dependence $E^C(\text{RAM})$ little sensitive to the geometry for RAMs much lower than the maximum possible RAM on a sphere at a given S (i.e. away from $L=0$). The general tendency is a decrease of E^C with increasing RAM (\sim area occupied by electrons), and the fine structure is associated with the magic states.

On a sphere, the lowest-LL degeneracy is $2S + 1$ (depends on S). However, at a fixed RAM, the electrons can only scatter to a fixed set of orbitals without violating the conservation of M and, hence, they are restricted to a certain area around the north pole. When S is increased at a fixed RAM, the diameter of the occupied area, scaled by the magnetic length, $l_B = \text{const.}$, becomes smaller and smaller compared to the sphere radius, R , and the curvature of the surface becomes less and less significant (cf. the approximate area occupied by electrons in the lowest-energy state at $\text{RAM} = 30$ for $2S = 50$, shaded in the inset in Fig. 2; see also Fig. 7 in Ref. [11]). Consequently, in the limit of $S \rightarrow \infty$, all relevant interaction matrix elements on a sphere converge to those on a plane. Also, at a high enough S , so that the conservation of M prevents scattering to the opposite (south) pole, the numbers of states in the RAM-space on a sphere and on a plane are equal. Hence, at each RAM, when S increases, the energy spectrum and wavefunctions on a sphere converge to those on a plane. The convergence of $E^C(\text{RAM})$ is clearly visible in Fig. 2.

¹ The minimum value of the Coulomb interaction energy for a given value of angular momentum L decreases as L increases, but not in a monotonic fashion. Downward cusps appear at certain values of L for which the Coulomb energy is particularly small. The confinement energy (in a parabolic quantum dot) increases linearly with L . The competition between these two energies determines the GS. Since the confinement energy can be varied by changing the parabolic potential, its slope as a function of L can be varied. Because of this, when two downward cusps are connected by a straight line, intermediate cusps which fall above this line will not be absolute minima for any value of the confining potential. This is the condition that determines the potential GSs. Note that the intermediate cusps falling between cusps marked as GSs in the figure all lie above a straight line connecting a pair of neighboring GSs. This effect is well known for ‘magic states’ of quantum dots. See, for example, Refs. [11–14].

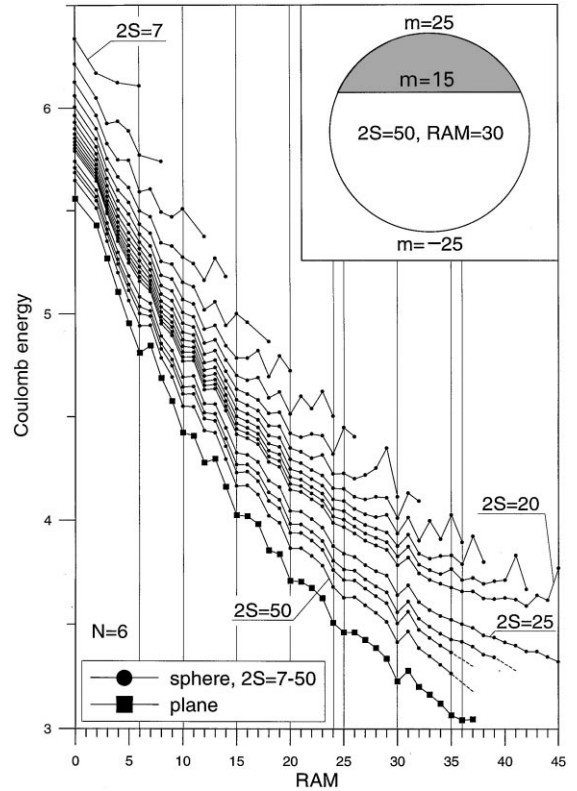


Fig. 2. Coulomb energy of six electrons on a sphere (dots) as a function of relative angular momentum (RAM). The series of curves correspond to magnetic monopoles of strength $2S = 7, 8, \dots, 20, 25, 30, 35$, and 50 . Energy is measured in units of $\langle SS|V_C|SS\rangle$. Squares give analogous dependence for a plane (vertical lines mark magic RAMs). Inset: approximate area occupied by electrons at $\text{RAM} = 30$ for $2S = 50$ (shaded).

The feature that is obviously unique for the sphere (closed surface) and does not occur on the plane (open surface) is the sensitivity of $E^C(\text{RAM})$ close to $L = 0$ ($\text{RAM} = L_{\text{CD}}$) to S and N . There are strong oscillations of E^C vs. RAM in the vicinity of $L = 0$, and whether the GS of interaction alone (for $\Delta = 0$) occurs at $L = 0$ or $L > 0$, depends on S and N (e.g., for $N = 6$, the $L = 0$ state for $2S = 15$ is the incompressible state with $\nu = 1/3$). This has been studied in a great detail in connection with the formation of composite fermions and the fractional quantum Hall effect [2,3,16–18].

A reason for that might appear to be the finite dimension of the SP space. While at $\text{RAM} \approx 0$ only a top part of the sphere is available for the electron scatter-

ing and the fact that the surface is closed is irrelevant, at $L \approx 0$ the limitation of available SP space becomes crucial. The SP space on a plane can be reduced to the same dimension as that of a sphere for a given S by keeping in hamiltonian H only these terms, which describe scattering to the SP states corresponding to those available on a sphere. The dependence of E^C on RAM obtained in this way is very similar to that for the complete SP space, which shows that the finite dimension of the SP space is of little importance. (Note, that reduction of the SP space is not equivalent to an introduction of a SP potential, and breaks the CM–REL separation.)

The true reason for the unique behavior of $E^C(\text{RAM})$ on a sphere close to $L = 0$ is the topological difference between an open and closed surface. The convergence of interaction matrix elements on a sphere is only a pointwise-like one, for each RAM $\lim_{S \rightarrow \infty} \langle V_C^{\text{sphere}} \rangle = \langle V_C^{\text{plane}} \rangle$, where $\langle V_C \rangle$ are all interaction matrix elements, which describe scattering allowed within a given RAM-space. The uniform-like convergence, $\lim_{S \rightarrow \infty}$ for each RAM ..., does not hold (e.g. $\langle S, -S | V_C^{\text{sphere}} | S, -S \rangle$ does not converge to any matrix element on a plane). Thus, an unconfined ($\Delta = 0$), edge-free, finite ($N < \infty$) system on the sphere is inherently different from a finite system on a plane, whose stability always requires a potential wall or an edge. Indeed, it is rather analogous to an infinite planar system with an equal density (which can be modeled, e.g. using PBC [4]).

5. Dependence of the excitation spectrum on the form of interaction potential

It is also interesting to compare the energy spectra obtained for different forms of the interaction potential [19]. So far we have used the Coulomb potential, $V_C \sim r_{ij}^\alpha$, where $\alpha = -1$. In Fig. 3 we compare the $E^C(\text{RAM})$ dependences obtained for six electrons on a sphere, at $2S = 15$ (the GS with $L = 0$ is the incompressible state with $\nu = 1/3$), for different values of α . To keep interaction repulsive, we flip the sign of V_C for $\alpha < 0$. Also, since the energy scales for different values of α are independent, and we are only interested in the magic values of RAM and the fine

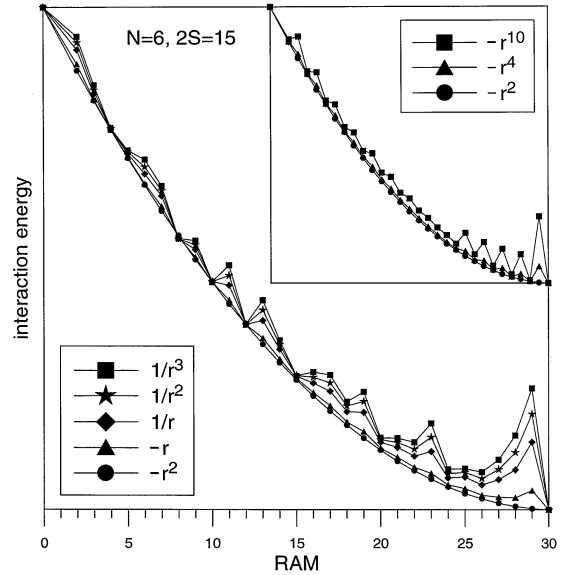


Fig. 3. Interaction energy of six electrons on a sphere for magnetic monopole strength $2S = 15$, as a function of relative angular momentum (RAM). Different curves correspond to different forms of the interaction potential, $V_C \sim r^\alpha$. Scale and zero on energy axes are different for each α . Main frame: $\alpha \leq 2$; inset: $\alpha \geq 2$.

structure of $E^C(\text{RAM})$ on top of the general, monotonic behaviour, the energy axis for each potential has been stretched and shifted so that the energies coincide at $\text{RAM} = 0$ and $\text{RAM} = 30$ ($L = 0$).

As seen in the main frame in Fig. 3, the fine structure in $E^C(\text{RAM})$ is virtually identical for different values of $\alpha < 2$, and only becomes more pronounced for lower α (partly due to the arbitrary scaling of the curves). In particular, neither the sequence of magic GS's nor the condensation into an incompressible $L = 0$ state depend on α , which means that all these interaction potentials favor virtually identical REL (eigen) states.

The harmonic interaction potential ($\alpha = 2$) gives a trivial $E^C(\text{RAM})$ dependence, since, within the lowest LL on a sphere, $\sum_{ij} r_{ij}^2/R^2 = N^2 - N/(S + 1) - L(L + 1)/(S + 1)^2$. Consequently, each RAM-space is degenerate, $E^C(\text{RAM})$ is a parabola, and the sequence of magic RAM's includes all values for which the given RAM-space is not empty. Also, the meaning of RAM as a quantum number characterizing

the REL motion (in the lowest LL) is now clarified: RAM measures the average squared distance between the particles. (This is also true for the plane, where $\sum_{ij} r_{ij}^2/l_B^2$ is linear in RAM [14,20]).

In the inset in Fig. 3, we show the $E^C(\text{RAM})$ dependences obtained for a few different values of $\alpha \geq 2$. Like in case of $\alpha < 2$, all interaction potentials for $\alpha > 2$ favor the same magic RAMs and thus virtually the same REL (eigen) states. However, these states are different from those for $\alpha < 2$.

The main conclusion from the above analysis is that repulsive interaction potentials in the form $V_C \sim r_{ij}^\alpha$ fall into three classes, leading to three distinct MP spectra:

(i) $\alpha < 2$; short-range potentials (in the limit of $\alpha \rightarrow \infty$, V_C acts like a delta-peak potential). They lead to the energy spectra, magic RAM's, incompressible states, composite-fermion formation, FQHE, etc., characteristic for the Coulomb interaction. Note that on a plane at $\nu = 1/m$ (m is an odd integer), Laughlin's states [3] become exact GS's in the limit of vanishing interaction range [19]. Also, on a sphere, the analogous Laughlin-like states become exact GSs of a 'hard-core interaction' defined by Haldane [2].

(ii) $\alpha = 2$; squared-distance (harmonic) potential. Interaction energy as a function of RAM is a parabola. This interaction does not lead to the incompressible states (the excitation gap vanishes in the thermodynamic limit of $S \rightarrow \infty$ at a constant ν).

(iii) $\alpha > 2$; these potentials act as if an electron were *attracted* by short-range potential to the other electron's antipole (antipole of an electron at $\hat{\Omega}$ is at $-\hat{\Omega}$). In the limit of $\alpha \rightarrow -\infty$, the potential of this attraction is a peak at $r_{ij} = 2R$. Also these interactions do not open the excitation gap at any ν . In the minimum-energy RAM = 0 state, half of electrons pack tightly around one pole, and the other half around the other pole. The system is somewhat similar to just two repelling electrons and, e.g., the REL states with even RAMs are favored.

6. Conclusion

In conclusion, we have demonstrated the correspondence between excitations and associated quantum

numbers of finite 2D electron systems in the lowest LL on a plane and on a sphere. Despite a coupling between CM and REL hamiltonians on a general surface (e.g. on a sphere), the class of CM excitations that do not couple to the REL motion have been identified. When the sphere radius increases while the magnetic field on the surface is fixed, the excitation spectrum has been shown to converge to that on a plane. In particular, when a (quantum-dot) lateral confinement is applied, the sequence of magic states on a sphere repeats that on a plane.

Also, a wide class of short-range interaction potentials have been shown to lead to the occurrence of incompressible GS's at special fractional filling factors, and thus to the FQHE in case of an extended system.

Acknowledgements

This work was supported in part by the Materials Research Program of Basic Energy Sciences, US Department of Energy. A.W. Thanks P. Hawrylak (IMS NRC Canada) and D.C. Marinescu (ORNL) for helpful discussions and acknowledges financial support from the KBN Grant No. PB674/P03/96/10.

References

- [1] D.C. Tsui, H.L. Störmer, A.C. Gossard, *Phys. Rev. Lett.* 48 (1982) 1559; *The Quantum Hall Effect*, R.E. Prange, S.M. Girvin (Eds.), Springer, New York, 1987.
- [2] F.D.M. Haldane, *Phys. Rev. Lett.* 51 (1983) 605.
- [3] R. Laughlin, *Phys. Rev. Lett.* 50 (1983) 1395.
- [4] F.D.M. Haldane, *Phys. Rev. Lett.* 55 (1985) 2095.
- [5] M. Kastner, *Phys. Today* 46 (1) (1993) 24; R.C. Ashoori, *Nature* 379 (1996) 413.
- [6] T.T. Wu, C.N. Yang, *Nucl. Phys. B* 107 (1976) 365; *Phys. Rev. D* 16 (1977) 1018.
- [7] P. Hawrylak, *Solid State Commun.* 88 (1993) 475.
- [8] G. Fano, F. Ortolani, E. Colombo, *Phys. Rev. B* 34 (1986) 2670.
- [9] A.H. MacDonald, S.R.E. Yang, M.D. Johnson, *Aust. J. Phys.* 46 (1993) 345; C. de Chamon, X.G. Wen, *Phys. Rev. B* 49 (1994) 8227.
- [10] P. Hawrylak, A. Wójs, J.A. Brum, *Solid State Commun.* 98 (1996) 847; *Phys. Rev. B* 54 (1996) 11 397.
- [11] A. Wójs, P. Hawrylak, *Phys. Rev. B* 56 (1997) 13 227.
- [12] P. Hawrylak, *Phys. Rev. Lett.* 71 (1993) 3347.
- [13] P. Maksym, T. Chakraborty, *Phys. Rev. Lett.* 65 (1990) 108.

- [14] L. Jacak, P. Hawrylak, A. Wójs, *Quantum Dots*, Springer, Berlin, 1998.
- [15] W. Kohn, *Phys. Rev.* 123 (1961) 1242; L. Brey, N.F. Johnson, B. Halperin, *Phys. Rev. B* 40 (1989) 10 647.
- [16] J. Jain, *Phys. Rev. Lett.* 63 (1989) 199.
- [17] P. Sitko, K.-S. Yi, J.J. Quinn, *Phys. Rev. B* 56 (1997) 12 417; P. Sitko, S.N. Yi, K.-S. Yi, J.J. Quinn, *Phys. Rev. Lett.* 76 (1996) 3396.
- [18] X.M. Chen, J.J. Quinn, *Solid State Commun.* 92 (1996) 865.
- [19] S.A. Trugman, S. Kivelson, *Phys. Rev. B* 31 (1985) 5280.
- [20] N.F. Johnson, M.C. Payne, *Phys. Rev. Lett.* 67 (1991) 1157.